

interactions are included.^{25,37} It would appear therefore that the N···N-type interactions are not essential to the force field and that in this case the poorer agreement is connected with the effects of lattice distortion. The angles in the ligand skeleton (Figure 3, Table III), apart from the distorted ring IV, are reproduced to within 0–2 standard deviations of the crystal values by both force fields. The calculation with set 1 force constants again has a better correlation, though for less crystal distorted complexes³⁷ better correlation is obtained using set 2. Both calculated and observed angles show that most angular strain occurs at the secondary nitrogen atoms where the ligand is turning from one chelate ring to the next. Bond angles of the types X–Y–H and H–X–H have a range 106.5–110.5°, with the vast majority very close to 109.5°. The lowest values are associated with the H–C–H angles of C₃, C₄, C₃', C₄'; not surprisingly these are the hydrogen atoms with the strong repulsive contacts in Table VII.

(37) The $\alpha\beta S$ and $\alpha\beta R$ isomers of chlorotetraethylenepentaminecobalt(III): M. R. Snow, manuscript in preparation.

This result justifies the procedure for adding the hydrogen atoms to the X-ray structure factor calculation.

The total strain energy of the complex ion at equilibrium was 20.21 (set 1), 20.93 (set 2), and 18.05 (set 2 omitting N···N and N···Cl nonbonded interactions) kcal/mol. This last strain energy is made up of E_r (1.08), E_θ (2.24), E_ϕ (7.7), and E_{nb} (7.02 kcal/mol) terms, of which the last two are most important. The distorted complex in the crystal has an energy of approximately 2.5 kcal/mol above the minimized strain energy calculated above. The major term is the unfavorable bond torsion energy (1.8 kcal/mol) of the envelope ring conformation. The usefulness of the strain energies in determining equilibria between isomers of metal complexes will be discussed elsewhere.^{25,37}

Acknowledgments. We thank Dr. P. Marzilli and A. M. Sargeson, and I. E. Maxwell for their continued interest, and Drs. Marzilli and Sargeson for the crystals used in this work. We also thank Professor R. H. Boyd for his minimization program, and the Australian Research Grants Committee for financial support.

Prediction of Molecular Geometries and Relative Stabilities in Chelate Complexes. Application to Cobalt(III) Triethylenetetramine-(*S*)-prolinato Complexes

D. A. Buckingham,^{1a} I. E. Maxwell,^{1a} A. M. Sargeson,^{1a} and M. R. Snow^{1b}

Contribution from the Research School of Chemistry, Australian National University, Canberra, Australia 2600, and the Department of Physical and Inorganic Chemistry, The University of Adelaide, Adelaide, South Australia 5000. Received November 7, 1969

Abstract: The technique of conformational potential energy minimization has been successfully applied to a series of β -[Co(trien)(*S*-Pro)]²⁺ complexes (trien = triethylenetetramine, *S*-Pro = L-proline). A general force field has been used including contributions from nonbonded interactions, bond angle bending, torsional potentials, and bond stretching. A modified Newton–Raphson method of minimization, due to Boyd, has been used to vary all the independent coordinates simultaneously. This method is superior to steepest descents techniques in that the parameter shifts are calculated directly. The calculated geometries of these strained molecules agree very well with the geometries obtained from crystal structure analysis studies. The method has been particularly successful in reproducing major angular distortions and the detailed conformations of the puckered chelate rings. Predicted energy differences between the isomers have been found to be in good agreement with experiment. The geometries and relative stabilities of other related isomers are predicted.

Although the techniques of minimization of conformational potential energy have been used for some time in organic chemistry it is only recently with the availability of high speed digital computers that the minimization techniques have greatly improved.^{2–5} A parallel improvement has occurred in our knowledge of potential functions particularly for bond length and

angular deformation force constants. However, throughout this development at no stage have cooperative minimization techniques been applied to inorganic structures, although some studies have been made on the conformational analysis of chelate systems.

The pioneering work of Mathieu⁶ and Corey and Bailar⁷ on chelate ring conformations indicated the importance of nonbonded interactions as a factor in determining isomer stabilities, and this was later supported by similar simple calculations and equilibrium measurements.⁸ One of the problems in these studies

(1) (a) Research School of Chemistry, Australian National University; (b) Department of Physical and Inorganic Chemistry, The University of Adelaide.

(2) (a) J. B. Hendrickson, *J. Amer. Chem. Soc.*, **83**, 4537 (1961); (b) K. B. Wiberg, *ibid.*, **87**, 1070 (1965).

(3) M. Bixon and S. Lifson, *Tetrahedron*, **23**, 769 (1967).

(4) E. J. Jacob, H. B. Thompson, and L. S. Bartell, *J. Chem. Phys.*, **47**, 3736 (1967).

(5) R. H. Boyd, *ibid.*, **49**, 2574 (1968).

(6) J. P. Mathieu, *Ann. Phys. (Paris)*, **19**, 335 (1944).

(7) E. J. Corey and J. C. Bailar, *J. Amer. Chem. Soc.*, **81**, 2620 (1959).

(8) A. M. Sargeson, "Transition Metal Chemistry," Vol. 3, R. L. Carlin, Ed., Marcel Dekker, New York, N. Y., 1966, p 303.

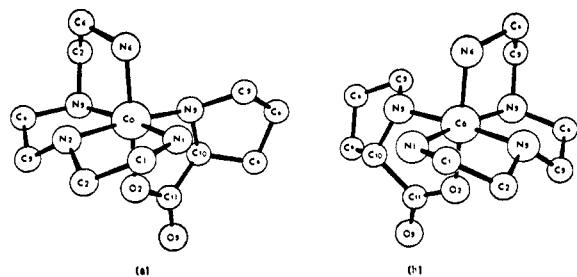


Figure 1. Perspective views of crystal structures: (a) $L\text{-}\beta_2\text{-(RRS)-[Co(trien)(S-Pro)]}^{2+}$, (b) $D\text{-}\beta_2\text{-(SSS)-[Co(trien)(S-Pro)]}^{2+}$ isomers.

was the absence of a precise knowledge of the molecular geometry in the molecules concerned and little was to be gained at that time by a more comprehensive approach. However, in the past few years X-ray analysis has provided accurate structural detail, and the calculation of minimum energy conformations of substituted five-membered diamine chelate rings has recently been reexamined.⁹ Although a general force field was used in this study, it was restricted to calculating the effect of one variable at a time on the total energy.⁹ The potential surface was then mapped for several changes in the variables. In the present paper the results of conformational energy minimization calculations on a number of isomeric chelate complexes are described where all the independent internal coordinates are allowed to vary simultaneously.

The complexes chosen were a series of $[\text{Co(trien)-(S-Pro)}]^{2+}$ ions (trien = 1,4,7,10 tetrazadecane, S-Pro = L-proline), two of which have been isolated.^{10,11} The study arose from a prediction that (S)-proline would react stereospecifically with racemic $\beta_2\text{-[Co(trien)-OH(OH}_2\text{)]}^{2+}$ to give exclusively $L\text{-}\beta_2\text{-(RRS)-[Co(trien)-(S-Pro)]}^{2+}$.¹¹ The prediction was based on a consideration of the nonbonded interactions in Dreiding models of the two most probable isomeric products, $L\text{-}\beta_2\text{-(RRS)-[Co(trien)(S-Pro)]}^{2+}$ and $D\text{-}\beta_2\text{-(SSS)-[Co(trien)(S-Pro)]}^{2+}$ (Figure 1). It was argued that the interactions between the proline ring and the neighboring apical trien chelate ring in the D isomer would be prohibitive and the effect would exert itself in the relative rates of formation of the proline complexes. It was puzzling, therefore, that practically all the reaction product was accounted for by approximately equal amounts of two $[\text{Co(trien)(S-Pro)}]^{2+}$ ions. Moreover, the rotatory dispersion and circular dichroism curves indicated that these ions were essentially catoptric in the arrangement of the ligands about the Co(III) ion. The structures of the two species were determined by X-ray methods as the $L\text{-}\beta_2\text{-(RRS)}$ and $D\text{-}\beta_2\text{-(SSS)}$ ions (Figure 1).¹¹⁻¹⁴

(9) J. R. Gologly and C. J. Hawkins, *Inorg. Chem.*, **8**, 1168 (1969).

(10) C. Lin and B. E. Douglas, *Inorg. Nucl. Chem. Lett.*, **4**, 15 (1968).

(11) D. A. Buckingham, L. G. Marzilli, I. E. Maxwell, and A. M. Sargeson, *Chem. Commun.*, 583 (1969).

(12) H. C. Freeman and I. E. Maxwell, *Inorg. Chem.*, in press.

(13) H. C. Freeman, L. G. Marzilli, and I. E. Maxwell, to be submitted for publication.

(14) Nomenclature: *R* and *S* designate the asymmetry about the "angular" and "planar" asymmetric N atoms of triethylenetetramine and the secondary N atom of the amino acid in that order, and follow the rules suggested by C. K. Ingold, V. Prelog, and R. S. Cahn, *Angew. Chem., Int. Ed. Engl.*, **5**, 385 (1966), and accepted by IUPAC. For consistency we have also used this nomenclature to specify the configuration of the $\alpha\text{-C}$ atom of the amino acid (e.g., *S*-proline = *L*-proline. The use of β , β_1 , and β_2 follows that used by L. G. Marzilli and D. A. Buckingham, *Inorg. Chem.*, **6**, 1042 (1967). The absolute configuration about the cobalt center is indicated by the prefix *L* or *D* (see above reference).

The X-ray technique also indicated that considerable internal strain existed in these molecules. These closely related ions of known structure were therefore ideally suited to a study of the effects of nonbonded interactions, valence deformations, bond length distortions, and torsional strain in determining molecular geometry and relative stabilities.

Potential Functions

The conformational potential energy, U , of a molecule was assumed to be equal to the summation of a number of terms, *i.e.*

$$U = \sum_{ij} U(r_{ij})_{\text{nb}} + \sum_{ijk} U(\theta_{ijk}) + \sum_{ijkl} U(\phi_{ijkl}) + \sum_{ij} U(r_{ij})_{\text{B}}$$

where $U(r_{ij})_{\text{nb}}$ is the nonbonded potential energy between two atoms *i* and *j*, $U(\theta_{ijk})$ is the potential energy for valence angle deformation between bonded atoms *i*, *j*, and *k*, $U(\phi_{ijkl})$ is the potential energy for torsional strain about the bond *jk* as defined by bonded atoms *i*, *j*, *k*, and *l*, and $U(r_{ij})_{\text{B}}$ is the potential energy for bond deformation between bonded atoms *i* and *j*. We shall consider each of these terms separately.

Nonbonded Potential Functions. The general form of the nonbonded potential function between a pair of atoms *i* and *j* is

$$U(r_{ij})_{\text{nb}} = \frac{a_{ij} \exp(-b_{ij}r_{ij})}{r_{ij}d_{ij}} - \frac{c_{ij}}{r_{ij}^6}$$

When $b_{ij} = 0$ and $d_{ij} = 12$ the function is of the Lennard-Jones type, and if $d_{ij} = 0$ the function reduces to the Buckingham type, *i.e.*

$$U(r_{ij})_{\text{nb}} = a_{ij} \exp(-b_{ij}r_{ij}) - c_{ij}/r_{ij}^6$$

In the calculations described in this paper we have used functions of the Buckingham form and constants given by De Coen, *et al.*¹⁵ (see Table I). These constants were obtained by comparing various calculated potential energy curves with experimental potential energy curves for gaseous molecules such as methane. The constants for oxygen and nitrogen nonbonded interactions are those listed by Liquori, *et al.*¹⁶

The potential functions using these constants lie somewhere between the "hard" Mason and Kreevoy functions¹⁷ and the "soft" Scott and Sheraga¹⁸ curves and close to the Bartell functions.¹⁹ All interactions between nonbonded atoms (except between atoms bonded to the same atom) up to distances of 1.2 times the sum of their van der Waals radii have been included.

Valence Angle Deformations and Bond Stretching Potential Functions. Both valence angle deformations and bond stretching potential functions have been assumed to be of the form

$$U(\theta_{ijk}) = \frac{1}{2}k_{ijk}(\theta_{ijk} - \theta_{ijk}^0)^2$$

for valence deformation and

$$U(r_{ij}) = \frac{1}{2}k_{ij}'(r_{ij} - r_{ij}^0)^2$$

(15) J. L. De Coen, G. Elefante, A. M. Liquori, and A. Damiani, *Nature*, **216**, 910 (1967).

(16) A. M. Liquori, A. Damiani, and G. Elefante, *J. Mol. Biol.*, **33**, 439 (1968).

(17) E. A. Mason and M. M. Kreevoy, *J. Amer. Chem. Soc.*, **77**, 5808 (1955).

(18) R. A. Scott and H. A. Sheraga, *J. Chem. Phys.*, **45**, 2091 (1966); *J. Mol. Biol.*, **33**, 439 (1968).

(19) L. Bartell, *J. Chem. Phys.*, **32**, 827 (1960).

Table I. Force Field Potential Function Constants^a

Nonbonded Potential Function Constants ^b				
Nonbonded atoms	a_{ij}	$b_{ij}, \text{\AA}^{-1}$	c_{ij}	Ref
H...H	45.8	4.08	0.341	15
C...H	218	4.20	0.84	15
N...H	195	4.32	0.69	16
C...C	1640	4.32	2.07	15
C...N	1472	4.44	1.695	16
N...N	1295	4.55	1.39	16
O...H	195	4.32	0.69	16
O...C	1472	4.44	1.695	16
O...N	1295	4.55	1.39	16
Bond Angle Force Constants, $k_{ijk}^{\theta, \phi}$				
Bond angle type	k_{ijk}^{θ}	θ_{ijk}° , radians		Ref
H—C—H	0.52	1.911		<i>d</i>
H—N—H	0.53	1.911		<i>e</i>
N—C—H	0.65	1.911		
C—N—H	0.56	1.911		
C—C—H	0.65	1.911		<i>d</i>
C—C—N	1.00	1.911		
N—Co—N	0.68	1.571		<i>e</i>
N—Co—O	0.68	1.571		<i>e</i>
Co—N—H	0.20	1.911		<i>e</i>
Co—N—C	0.40	1.911		
C—N—C	1.0	1.911		
C—C—C	1.0	1.911		<i>d</i>
O—C—O	1.0	2.095		
O—C—C	1.0	2.095		
Co—O—C	0.40	2.095		
Bond Length Force Constants ^c				
Bond type	k_{ij}^r	r_{ij}° , \AA		Ref
N—H	5.6	1.03		<i>e</i>
C—H	5.0	1.09		<i>d</i>
C—C	5.0	1.50		<i>d</i>
C—N	6.0	1.49		
Co—N	1.75	1.925		<i>e</i>
Co—N	1.75	1.90		
C=O	9.0	1.24		<i>f</i>

^a Constants which are not referenced have been estimated and in some instances fitted to give best agreement with the structural data. ^b The units for parameters a_{ij} and c_{ij} , respectively, are 10^{-11} erg molecule⁻¹ and 10^{-11} erg \AA⁶ molecule⁻¹. ^c Force constants are given in 10^6 dyn cm⁻¹. ^d J. H. Schachtschneider and R. G. Snyder, *Spectrochim. Acta*, **19**, 117 (1963). ^e I. Nakagawa and T. Shimanouchi, *ibid.*, **22**, 759, 1707 (1966). ^f O. Thomas, *Discuss. Faraday Soc.*, No. 9, 339 (1950).

for bond stretching, where θ_{ijk}° and r_{ij}° are the unstrained values for valence deformation and bond stretching, respectively, and k_{ijk}^{θ} and k_{ij}^r are the force constants for angle deformation and bond stretching, respectively. The various constants used are listed in Table I. Angle deformation and bond stretching terms have been included for all bond angles and bonds within the molecule.

Torsional Potential Energy. The general expression for a threefold potential barrier is a Fourier series of the form²⁰

$$U(\phi) = (V_3/2)(1 + \cos 3\phi) + (V_6/2)(1 + \cos 6\phi) + (V_9/2)(1 + \cos 9\phi) + (V_{12}/2)(1 + \cos 12\phi) + \dots \quad (1)$$

where $V_3 \gg V_6 \gg V_9 \gg V_{12}$.

For molecules like ethane and methylamine, since V_6 is very much smaller than V_3 ,²⁰ it is not possible experimentally to get a reliable estimate of V_6 . Hence,

(20) D. J. Millen, *Progr. Stereochem.*, **3**, 138 (1962).

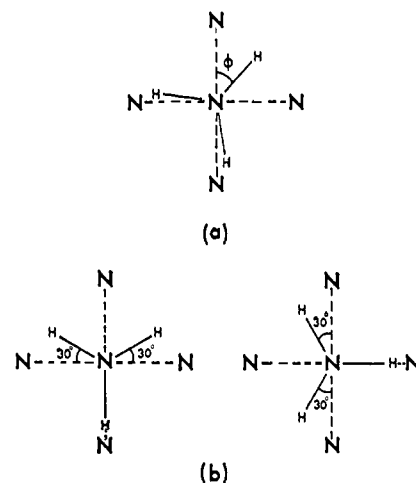


Figure 2. Projections down the Co-N bond for $[\text{Co}(\text{NH}_3)_6]^{3+}$ showing (a) torsion angle ϕ , (b) 12-fold symmetry.

for most purposes only the V_3 term is considered. In the calculations described here, the V_3 torsional barriers about C-C (2.4 kcal/mol) and C-N (1.54 kcal/mol) bonds were determined by subtracting out the nonbonded contributions from the observed rotational barriers in ethane and methylamine, respectively.²⁰

Hawkins and Gollogly⁹ recently considered the torsional barriers to rotation about a coordinate bond. They assumed the barrier to be described by a simple threefold potential and derived an expression for the rotational barrier about the Co-N bond in hexaamminecobalt(III) ion as

$$U(\phi) = \sum_{i=1}^4 (V_i/2)[1 + \cos 3(\phi + (i-1)90)] \quad (2)$$

where ϕ is the torsional angle as shown in Figure 2a. However, the rotational symmetry about the Co-N bond is not simply threefold but is 12-fold since rotation by 30° gives an identical configuration (see Figure 2b). Thus it can be shown that the first term in eq 1 with a nonvanishing periodicity will be the V_{12} term. This follows directly from the rotational symmetry about the bond. The rotational potential about the Co-N bond in cobalt hexaammine can then be represented by

$$U(\phi) = (V_{12}/2)(1 + \cos 12\phi)$$

This rotational barrier (V_{12}) must be extremely small owing to the known rapid falloff of the coefficients in the Fourier series. For example, in nitromethane the first term with nonvanishing periodicity is the sixfold term, where the barrier V_6 is 0.006 kcal/mol²⁰ and the V_{12} barrier has been estimated to be less than 5×10^{-5} kcal/mol.²⁰ In general if the periodicity is large the energy difference between maxima and minima will be smaller than for the threefold case. This arises primarily because the minima are never far from positions of eclipse and at the maxima complete eclipse does not occur as with superimposed threefold rotors. These arguments imply a small barrier for the complexes discussed later. The contributions from nonbonded interactions in the torsional barrier are included separately and the results support the conclusion that the torsional term alone is negligible.

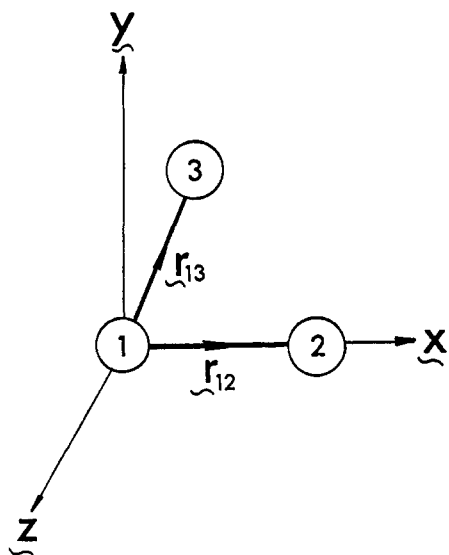


Figure 3. Standard reference Cartesian coordinate system.

Minimization Method

The Mathematical Method. We have adopted the energy minimization method of Boyd,⁵ which is a modified Newton-Raphson method. The gradient of the total conformational potential energy, $\nabla U(\mathbf{r})$ (where \mathbf{r} now represents atomic coordinates), is expanded in a Taylor series at a point near equilibrium. Then

$$\nabla U(\mathbf{r}_0) = \nabla U(\mathbf{r}) + \mathbf{F}(\mathbf{r})\delta\mathbf{r} \quad (3)$$

where \mathbf{r}_0 represents the equilibrium coordinates and $\mathbf{F}(\mathbf{r})$ is the matrix of second derivatives, *i.e.*

$$\mathbf{F}_{\alpha\beta} = \frac{\partial^2 U}{\partial r_\alpha \partial r_\beta}$$

The solution of the set of equations

$$\partial U / \partial r_\alpha = 0$$

represents the necessary but not sufficient condition that \mathbf{r}_0 is an equilibrium conformation; thus $\nabla U(\mathbf{r}_0) = 0$ and the equilibrium conformation is obtained by solving a set of linear equations for \mathbf{r}_0 as follows

$$\mathbf{r}_0 = \mathbf{r} + \delta\mathbf{r}$$

and therefore

$$\mathbf{r}_0 = \mathbf{r} - \mathbf{F}^{-1}\nabla U(\mathbf{r}) \quad (4)$$

However, eq 3 is approximate since cross terms are neglected and the expansion is truncated past second-order terms. Also eq 4 is normally solved in terms of Cartesian coordinates, and the equations of transformation from internal coordinates are approximated by assuming $\delta\mathbf{r}$ to be small. Thus the solution to eq 4 is not exact and the process of forming a set of linear equations is repeated using the new coordinates. After each iteration the coordinate shifts $\delta\mathbf{r}$ become smaller quantities until the problem converges and the $\delta\mathbf{r}$ become negligibly small. The minimization is considered converged when the root-mean-square displacement is less than 0.01 Å.

This minimization method is superior to the steepest descent technique in that the new set of displacements is calculated directly from the linear equations resulting

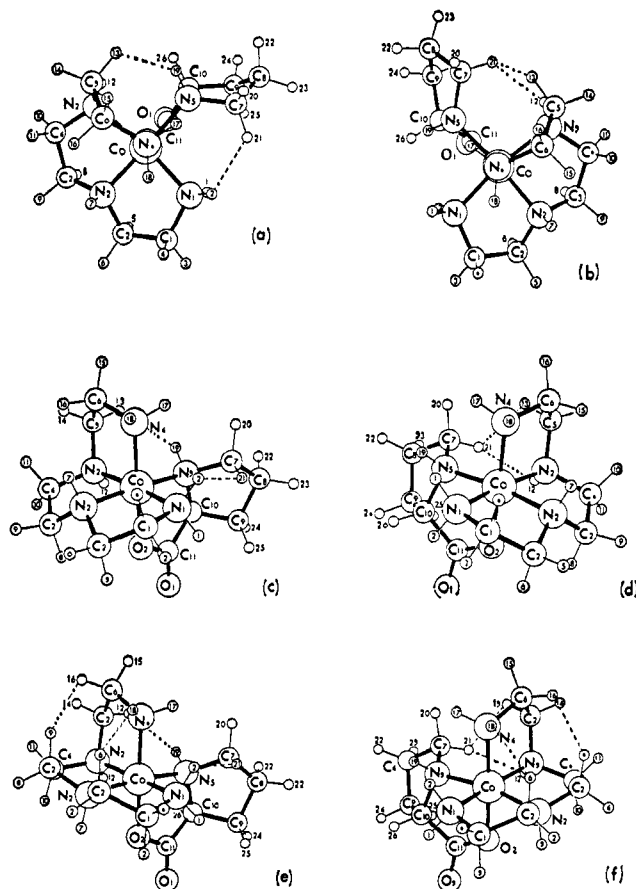


Figure 4. Perspective views of minimized complexes. Dashed lines indicate major H...H nonbonded interactions: (a) and (c) L- β_2 -(RRS)-[Co(trien)(S-Pro)]²⁺ ion, (b) and (d) D- β_2 -(SSS)-[Co(trien)(S-Pro)]²⁺ ion, (e) L- β_2 -(RSS)-[Co(trien)(S-Pro)]²⁺ ion, (f) D- β_2 -(SRS)-[Co(trien)(S-Pro)]²⁺ ion.

from differentiation and convergence is faster near the minimum.²¹

Invariant Internal Coordinates. In this minimization process, molecular translational and rotational degrees of freedom are not considered. Hence, at the most there are only $3N - 6$ degrees of freedom. The method of minimization described above uses Cartesian coordinates as trial molecular coordinates, and therefore six of these coordinates must be fixed. Where possible it is advantageous to extract trial coordinates from a crystal structure analysis. In this instance an independent internal coordinate may be invariant. To avoid this problem we have orthogonalized and reoriented our starting coordinate systems such that there are no invariant internal coordinates.

Arbitrarily, and necessarily, the coordinates $x_1, y_1, z_1, y_2, z_2,$ and z_3 are fixed during the minimization. If the reference coordinate system is defined as follows

$$\mathbf{x} = \mathbf{r}_{12}$$

$$\mathbf{y} = (\mathbf{r}_{12}\mathbf{r}_{13})\mathbf{r}_{12}$$

$$\mathbf{z} = \mathbf{r}_{12}\mathbf{r}_{13}$$

where the origin, 0, is at atom 1, then \mathbf{r}_{12} is the vector along the bond joining atoms 1 and 2 and \mathbf{r}_{13} is the vector along the bond joining atoms 1 and 3 (see Figure 3). In this way all six fixed coordinates are zero and

(21) S. Lifson and A. Warshel, *J. Chem. Phys.*, **49**, 5116 (1968).

Table II. Positional Coordinates (Å) of β_2 -[Co(trien)(S-Pro)]²⁺ Isomers from Energy Minimization

Atom	$L\text{-}\beta_2\text{(RRS)-[Co(trien)(S-Pro)]}^{2+}$			$D\text{-}\beta_2\text{(SSS)-[Co(trien)(S-Pro)]}^{2+}$			$L\text{-}\beta_2\text{(RSS)-[Co(trien)(S-Pro)]}^{2+}$			$D\text{-}\beta_2\text{(SRS)-[Co(trien)(S-Pro)]}^{2+}$		
	x	y	z	x	y	z	x	y	z	x	y	z
Co	0.000	0.000	0.000	0.000	0.000	0.000	0.000	0.000	0.000	0.000	0.000	0.000
N(1)	1.959	0.000	0.000	1.962	0.000	0.000	1.963	0.000	0.000	1.965	0.000	0.000
N(2)	0.118	1.928	0.000	0.128	1.928	0.000	0.157	1.930	0.000	0.187	1.927	0.000
N(3)	-1.942	0.279	-0.007	-1.944	0.288	0.017	-1.938	0.284	-0.156	-1.939	0.296	0.182
N(4)	-0.064	-0.100	-1.946	-0.058	-0.096	-1.948	-0.009	-0.239	-1.949	0.023	-0.269	1.945
N(5)	-0.197	-1.965	0.170	0.016	-1.975	-0.169	-0.177	-1.955	0.317	0.004	-1.957	-0.321
O(1)	-0.269	-1.154	3.695	0.415	-1.170	-3.667	0.031	-0.907	3.776	0.303	-0.893	-3.755
O(2)	0.012	-0.005	1.904	-0.006	-0.020	-1.906	-0.059	0.133	1.898	-0.097	0.110	-1.901
C(1)	2.454	1.412	-0.054	2.458	1.408	0.099	2.473	1.405	0.117	2.510	1.396	0.070
C(2)	1.433	2.294	0.603	1.454	2.295	-0.578	1.486	2.324	-0.547	1.468	2.306	0.660
C(3)	-1.044	2.429	0.790	-1.022	2.427	-0.807	-1.018	2.514	-0.698	-1.028	2.559	0.579
C(4)	-2.266	1.723	0.271	-2.252	1.731	-0.293	-2.215	1.765	-0.172	-2.196	1.773	0.044
C(5)	-2.432	-0.123	-1.367	-2.428	-0.062	1.395	-2.398	-0.372	-1.425	-2.384	-0.214	1.524
C(6)	-1.426	0.330	-2.391	-1.400	0.389	2.396	-1.391	-0.134	-2.515	-1.313	0.016	2.552
C(7)	0.896	-2.887	-0.283	-1.195	-2.810	0.105	0.818	-2.905	-0.288	-1.213	-2.793	-0.081
C(8)	0.792	-4.073	0.630	-0.987	-4.041	-0.725	1.124	-3.915	0.781	-1.038	-3.966	-0.997
C(9)	0.468	-3.453	1.955	-0.428	-3.492	-2.004	1.007	-3.129	2.050	-0.498	-3.338	-2.247
C(10)	-0.445	-2.302	1.612	0.415	-2.315	-1.576	-0.164	-2.221	1.793	0.361	-2.196	-1.759
C(11)	-0.143	-1.100	2.462	0.168	-1.119	-2.452	-0.017	-0.926	2.537	0.088	-0.938	-2.534
H(1)	2.310	-0.454	0.856	2.321	-0.547	0.797	2.313	-0.557	0.794	2.306	-0.447	-0.863
H(2)	2.323	-0.499	-0.824	2.320	-0.421	-0.869	2.331	-0.399	-0.876	2.317	-0.545	0.801
H(3)	3.409	1.496	0.469	3.429	1.503	-0.392	2.577	1.675	1.169	2.770	1.742	-0.933
H(4)	2.594	1.721	-1.092	2.562	1.698	1.146	3.447	1.495	-0.368	3.410	1.417	0.689
H(5)	1.433	2.120	1.680	1.680	3.344	-0.377	1.707	3.361	-0.289	1.711	3.346	0.434
H(6)	1.660	3.344	0.408	1.473	2.120	-1.654	1.525	2.211	-1.630	1.414	2.185	1.741
H(7)	0.069	2.310	-0.956	0.065	2.313	0.954	0.121	2.254	0.979	0.250	2.230	-0.985
H(8)	-0.918	2.224	1.854	-0.886	2.212	-1.867	-1.107	3.574	-0.452	-1.101	3.596	0.243
H(9)	-1.150	3.507	0.653	-1.124	3.507	-0.680	-0.923	2.417	-1.777	-1.001	2.555	1.665
H(10)	-3.060	1.783	1.018	-2.609	2.262	0.592	-2.424	2.101	0.845	-2.329	2.014	-1.012
H(11)	-2.612	2.235	-0.628	-3.036	1.784	-1.051	-3.087	1.997	-0.786	-3.106	2.065	0.571
H(12)	-2.380	-0.319	0.710	-2.404	-0.303	-0.690	-2.414	-0.150	0.650	-2.450	-0.191	-0.570
H(13)	-2.557	-1.203	-1.428	-2.584	-1.133	1.500	-2.534	-1.443	-1.279	-2.615	-1.276	1.480
H(14)	-3.402	0.333	-1.574	-3.383	0.426	1.601	-3.365	0.030	-1.732	-3.298	0.293	1.840
H(15)	-1.659	-0.123	-3.357	-1.405	1.476	2.480	-1.523	-0.891	-3.291	-1.478	-0.663	3.392
H(16)	-1.463	1.414	-2.502	-1.636	-0.032	3.376	-1.556	0.838	-2.977	-1.361	1.030	2.946
H(17)	0.114	-1.063	-2.263	0.081	-1.064	2.270	0.368	-1.170	-2.173	0.262	-1.253	2.134
H(18)	0.648	0.515	-2.366	0.679	0.492	2.365	0.594	0.454	-2.411	0.734	0.310	2.410
H(19)	-1.041	-2.221	-0.360	0.766	-2.298	0.461	-1.104	-2.228	-0.030	0.767	-2.339	0.259
H(20)	0.748	-3.194	-1.320	-1.264	-3.070	1.163	0.390	-3.407	-1.158	-1.266	-3.122	0.959
H(21)	1.881	-2.443	-0.170	-2.107	-2.321	-0.229	1.733	-2.401	-0.586	-2.121	-2.267	0.365
H(22)	-0.011	-4.739	0.307	-0.273	-4.713	-0.247	0.395	-4.727	0.763	-0.323	-4.678	-0.580
H(23)	1.738	-4.617	0.674	-1.932	-4.558	-0.902	2.133	-4.314	0.664	-1.993	-4.459	-1.188
H(24)	-0.041	-4.171	2.600	0.184	-4.243	-2.506	0.807	-3.790	2.896	0.101	-4.059	-2.808
H(25)	1.380	-3.101	2.441	-1.238	-3.177	-2.665	1.919	-2.558	2.232	-1.317	-2.978	-2.872
H(26)	-1.487	-2.595	1.760	1.474	-2.582	-1.617	-1.091	-2.711	2.101	1.417	-2.458	-1.852

the condition for complete variance of internal coordinates is satisfied. A general program has been written in FORTRAN to calculate Cartesian coordinates, based on this reference system, from triclinic (or higher symmetry) crystal coordinates.

Trial Coordinates. In all the molecules minimized in this paper, all or part of the trial molecular coordinates have been derived from crystal structure coordinates. Clearly, the better the trial coordinates the faster the convergence and the lesser is the chance of falling into false minima. The crystal coordinates were orthogonalized, with a new Cartesian reference system defined in the manner described in the previous section (hereafter called standardized coordinates).

Dampening Factors. In some instances large oscillations or even divergence occurred during refinement. This generally occurred when the starting coordinates were distant from the minimized coordinates and the number of parameters to be refined was large. The problem arose through over calculation of the parameter shifts, δr , and was remedied by incorporating a dampening factor, λ ($0 < \lambda \leq 1$), as a multiplier to the δr after each cycle. The new δr 's ($\delta r' = \lambda \delta r$) were then used to

calculate the starting coordinates for the subsequent cycle.

The values of λ chosen at any stage were dependent upon the distance of the trial coordinates from the minimum. Typically, the minimization of a large problem from a set of poor trial coordinates was started with a small value of λ (0.25). This was increased stepwise as the refinement progressed, reaching unity in the last few cycles. The procedure was successful in solving problems of oscillation or divergence. Moreover, the range of trial coordinates has been usefully extended, particularly for the larger minimization problems.

Results and Discussion

$L\text{-}\beta_2\text{(RRS)-[Co(trien)(S-Pro)]}^{2+}$ and $D\text{-}\beta_2\text{(SSS)-[Co(trien)(S-Pro)]}^{2+}$. The trial coordinates for the energy minimization of both $L\text{-}\beta_2\text{(RRS)-[Co(trien)(S-Pro)]}^{2+}$ and $D\text{-}\beta_2\text{(SSS)-[Co(trien)(S-Pro)]}^{2+}$ isomers were crystal structure coordinates,^{12,13} orthogonalized and standardized. Convergence from these trial coordinates was quite rapid (five-six cycles) and the final coordinates are shown in Table II. The summation

Table III. Comparison of Bond Angles in β_2 -[Co(trien)(S-Pro)]²⁺ Isomers

Atoms	L- β_2 -(RRS)		D- β_2 -(SSS)		L- β_2 -(RSS)	D- β_2 -(SRS)
	Minimization ^a	Crystal ^b	Minimization ^a	Crystal ^b	Minimization ^c	Minimization ^c
N(1)-Co-N(2)	86.5	85.5 (9)	86.2	85.5 (4)	85.3	84.4
N(2)-Co-N(3)	85.3	85.8 (9)	85.4	84.5 (3)	86.3	86.9
N(3)-Co-N(4)	88.3	86.2 (8)	88.2	85.8 (4)	86.2	86.6
O(2)-Co-N(5)	84.9	85.7 (7)	84.5	84.8 (3)	84.7	84.0
N(1)-Co-N(4)	91.9	92.2 (8)	91.7	93.9 (4)	90.3	89.3
N(2)-Co-N(4)	93.0	93.6 (8)	92.9	91.4 (4)	97.0	97.8
N(1)-Co-N(5)	95.7	94.6 (9)	89.5	90.9 (4)	95.1	89.9
N(5)-Co-N(4)	91.8	91.4 (8)	92.1	93.0 (4)	92.2	91.4
N(1)-Co-O(2)	89.6	90.2 (8)	90.2	90.4 (4)	91.8	92.9
N(2)-Co-O(2)	90.1	89.3 (7)	90.6	91.1 (3)	86.2	87.0
N(3)-Co-O(2)	90.6	91.8 (7)	90.4	90.3 (4)	92.2	91.9
N(3)-Co-N(5)	92.4	94.2 (9)	98.9	99.2 (4)	93.9	99.5
Co-N(1)-C(1)	109.3	110.4 (1.6)	109.3	110.7 (7)	109.9	111.3
N(1)-C(1)-C(2)	108.3	107.6 (2.1)	107.7	107.6 (1.0)	108.4	109.2
C(1)-C(2)-N(2)	106.2	104.9 (1.9)	105.9	106.5 (8)	105.1	105.6
C(2)-N(2)-Co	107.4	108.6 (1.4)	107.7	108.7 (7)	109.6	109.6
Co-N(2)-C(3)	106.7	108.2 (1.6)	106.4	107.4 (7)	109.1	110.1
N(2)-C(3)-C(4)	107.0	104.7 (1.9)	106.9	105.9 (9)	105.6	105.9
C(2)-N(2)-C(3)	113.0	111.3 (1.9)	113.2	115.8 (9)	115.4	115.0
C(3)-C(4)-N(3)	109.8	107.5 (1.9)	110.2	110.5 (1.0)	110.2	110.4
C(4)-N(3)-Co	110.4	109.4 (1.7)	109.9	110.9 (7)	108.9	107.9
Co-N(3)-C(5)	106.8	108.8 (1.3)	107.0	109.0 (7)	107.8	108.9
N(3)-C(5)-C(6)	108.5	106.6 (1.9)	108.7	106.8 (9)	109.8	110.3
C(5)-C(6)-N(4)	108.6	107.9 (1.9)	108.5	107.7 (9)	109.5	109.3
C(6)-N(4)-Co	108.2	109.6 (1.4)	108.1	110.2 (7)	111.7	111.4
Co-N(5)-C(10)	108.7	109.1 (1.3)	107.9	107.5 (6)	109.3	108.2
N(5)-C(7)-C(8)	104.6	104.5 (2.0)	104.1	103.3 (9)	105.9	104.1
C(7)-C(8)-C(9)	103.0	102.0 (2.0)	102.9	103.7 (9)	103.6	102.9
C(8)-C(9)-C(10)	104.2	98.9 (1.7)	104.6	103.4 (9)	103.5	104.6
C(9)-C(10)-N(5)	106.8	108.2 (1.8)	107.1	106.8 (8)	106.4	107.1
C(10)-N(5)-C(7)	105.8	104.2 (1.7)	105.1	105.2 (8)	106.1	105.0
Co-N(5)-C(7)	120.7	122.2 (1.7)	122.2	125.3 (7)	119.9	121.6
C(9)-C(10)-C(11)	111.1	111.9 (2.0)	111.3	114.4 (9)	111.1	111.3
N(5)-C(10)-C(11)	109.3	107.6 (1.8)	108.8	110.2 (9)	109.6	108.6
C(10)-C(11)-O(1)	120.5	118.2 (2.3)	120.3	121.6 (1.0)	120.8	120.4
C(10)-C(11)-O(2)	118.5	118.1 (2.0)	118.2	115.5 (9)	118.7	118.2
O(1)-C(11)-O(2)	119.9	123.4 (2.5)	119.7	123.0 (1.0)	120.3	119.9
Co-O(2)-C(11)	116.9	118.0 (1.6)	116.7	116.2 (6)	117.0	116.9
Comparison of Cobalt-Ligand Bond Lengths in β_2 -[Co-(trien)(S-Pro)] ²⁺ Isomers						
Co-N(1)	1.959	1.957 (18)	1.962	1.960 (9)	1.964	1.965
Co-N(2)	1.932	1.924 (21)	1.932	1.943 (8)	1.936	1.936
Co-N(3)	1.962	1.965 (19)	1.965	1.961 (9)	1.966	1.970
Co-N(4)	1.949	1.963 (17)	1.951	1.955 (9)	1.964	1.963
Co-N(5)	1.983	1.973 (21)	1.982	1.980 (9)	1.988	1.984
Co-O(2)	1.904	1.880 (14)	1.906	1.924 (7)	1.903	1.907

^a Results from energy minimization calculation. ^b Values determined from X-ray crystal structure analyses. ^c Nomenclature abbreviations: D- β_2 -(SSS) = D- β_2 -(SSS)-[Co(trien)(S-Pro)]²⁺, L- β_2 -(RRS) = L- β_2 -(RRS)-[Co(trien)(S-Pro)]²⁺, L- β_2 -(RSS) = L- β_2 -(RSS)-[Co(trien)(S-Pro)]²⁺, D- β_2 -(SRS) = D- β_2 -(SRS)-[Co(trien)(S-Pro)]²⁺.

of total energy (see eq 1) included 316 and 319 terms for the L-(RRS) and D-(SSS) forms, respectively. In each case a total of 129 independent coordinates was varied.

Perspective views of the molecules, accurately drawn from the minimized coordinates under computer control, are shown in Figure 4. Nonbonded interactions greater than 0.5 kcal/mol are shown as dashed lines.

Bond angles along with Co-N bond lengths from energy-minimized and crystal structure coordinates are compared in Table III. The numerous bond angles containing the H atoms do not vary greatly ($\pm 2^\circ$) and therefore are not listed. Also the intraligand bond lengths did not vary significantly from the unstrained values. However, the Co-N values did vary slightly and these appear in Table III.

The major angular distortions found in the crystals are accurately predicted from the minimization. The Co-N(5)-C(7) angles are L-(RRS), crystal, 122.2 (1.7) $^\circ$, minimization, 120.7 $^\circ$, 1.1 kcal/mol, and D-(SSS), crystal, 125.3 (0.7) $^\circ$, minimization, 122.2 $^\circ$, 1.4 kcal/mol (un-

strained value 109.5 $^\circ$). These large angular deformations considerably reduce H \cdots H repulsions and the final result is a balance between repulsive and angular energy terms.

The major geometrical difference between the L-(RRS) and D-(SSS) isomers is the relative orientation of the proline ring (see Figures 4a and 4b). In the L-(RRS) isomer the geometry is such that nonbonded repulsions between the extremities of trien and each side of the proline ring approximately balance. The major terms are H(2) \cdots H(21), 2.10 Å, 0.7 kcal/mol, and H(13) \cdots H(19), 2.12 Å, 0.63 kcal/mol (see Figure 4a), whereas for the D-(SSS) isomer the proline ring now interacts largely with the apical β -trien chelate ring. To alleviate this interaction the N(3)-Co-N(5) angle expands, thereby reducing the nonbonded interactions from prohibitive values (~ 14 kcal/mol) to much smaller quantities, *i.e.*, H(21) \cdots H(12), 2.09 Å, 0.7 kcal/mol, and H(21) \cdots H(13), 2.15 Å, 0.5 kcal/mol (see Figure 4b). The agreement between crystal structure and minimiza-

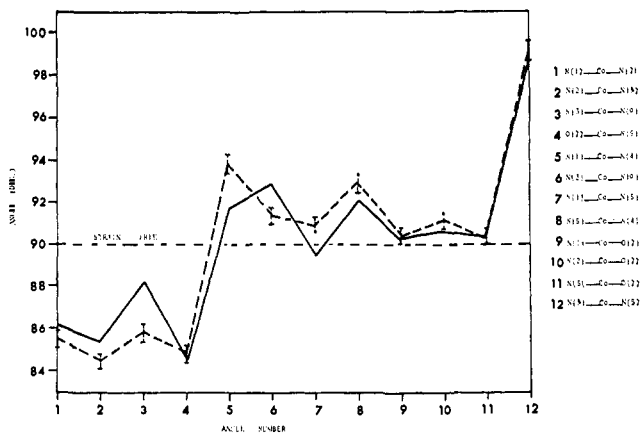


Figure 5. Comparison of bond angles about cobalt for $D\text{-}\beta_2\text{-(SSS)-[Co(trien)(S-Pro)]}^{2+}$; —, calculated from minimized coordinates; - - - -, calculated from crystal structure coordinates with standard deviations.

tion for the angular distortion is excellent, $N(3)\text{-Co-N}(5)$, crystal, $99.2(0.4)^\circ$; minimization, 98.9° , requiring 1.2 kcal/mol of strain energy from the unstrained value of 90° .

From Table III it is evident that the variation of angles about the coordination octahedron from the strain-free 90° value is quite large. Figure 5 compares the coordination angles calculated from crystal and minimization coordinates for the $D\text{-(SSS)}$ isomer. Clearly, the correlation indicates that these angles are primarily determined by the restrictions of coupled chelate geometry and nonbonded repulsions.

Comparison of $L\text{-}\beta_2\text{-(RSS)-[Co(trien)(S-Pro)]}^{2+}$ and $D\text{-}\beta_2\text{-(SRS)-[Co(trien)(S-Pro)]}^{2+}$. The $L\text{-(RSS)}$ and $D\text{-(SRS)}$ isomers differ from their related pairs $L\text{-(RRS)}$ and $D\text{-(SSS)}$, respectively, only in the orientation of groups about the asymmetric secondary nitrogen atom $N(2)$. Mutarotation at asymmetric N centers of this type have been observed in mildly basic solutions^{22,23} ($\text{pH} > 7$). No crystal structure data are available at present for trien coordinated in the $\beta\text{-SR}$ or $\beta\text{-RS}$ forms and therefore this aspect of the study is purely predictive.

The trial coordinates were derived by combining pieces of crystal structure data. The $\beta\text{-SR}$ and $\beta\text{-RS}$ trien moieties were obtained by extracting the appropriate coordinates from a related quinquidentate structure, 4-(2-aminoethyl)-1,4,7,10-tetraazadecaneazidocobalt(III) nitrate hydrate.²⁴ Proline was obtained from the $L\text{-(RRS)}$ and $D\text{-(SSS)}$ crystal structure coordinates.^{12,13} If both sets of crystal coordinates are in the orthogonalized standardized form with a common reference system, then the coordinates can be simply combined together.

Minimization of both these forms was somewhat slower (eight-ten cycles) owing to the poorer initial models. The final minimized coordinates are given in Table II. The energy summation included 318 and 320 terms for the $L\text{-(RSS)}$ and $D\text{-(SRS)}$ isomers, respectively. Perspective views of these molecules drawn

(22) D. A. Buckingham, P. A. Marzilli, and A. M. Sargeson, *Inorg. Chem.*, **6**, 1032 (1967).

(23) D. A. Buckingham, I. E. Maxwell, and A. M. Sargeson, *Chem. Commun.*, 581, (1969).

(24) D. A. Buckingham, H. C. Freeman, P. A. Marzilli, I. E. Maxwell, and A. M. Sargeson, *ibid.*, 473 (1969).

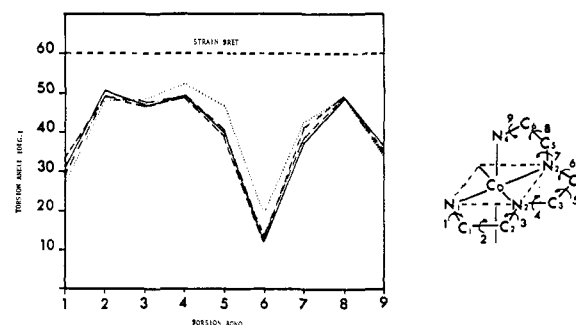


Figure 6. Comparison of torsional angles for trien chelate rings: —, calculated from minimized coordinates for $D\text{-}\beta_2\text{-(SSS)-[Co(trien)(S-Pro)]}^{2+}$; - - - -, calculated from crystal structure coordinates for $D\text{-}\beta_2\text{-(SSS)-[Co(trien)(S-Pro)]}^{2+}$; —, calculated from minimized coordinates for $L\text{-}\beta_2\text{-(RRS)-[Co(trien)(S-Pro)]}^{2+}$; - - - -, calculated from crystal structure coordinates for $L\text{-}\beta_2\text{-(RRS)-[Co(trien)(S-Pro)]}^{2+}$.

from the minimized coordinates are shown in Figure 4e and f. Intramolecular bond angles (excluding those involving H atoms), calculated from the minimized coordinates, are presented in Table III. Major angular distortions ($\text{Co-N}(5)\text{-C}(7)$ and $\text{N}(3)\text{-Co-N}(5)$ angles) and nonbonded repulsions involving the proline moiety are analogous to the $L\text{-(RRS)}$ and $D\text{-(SSS)}$ isomers. This is not surprising since the geometric environment around the proline is not significantly affected by inversion at the secondary nitrogen atom $N(2)$.

However, repulsive interactions within the trien rings become important. The major repulsive terms are $L\text{-(RSS)}$, $\text{H}(6)\cdots\text{H}(18)$, 2.14 Å, 0.6 kcal/mol; $\text{H}(9)\cdots\text{H}(16)$, 2.08 Å, 0.7 kcal/mol; and $D\text{-(SRS)}$, $\text{H}(6)\cdots\text{H}(18)$, 2.10, 0.7 kcal/mol; $\text{H}(9)\cdots\text{H}(16)$, 2.02 Å, 1.0 kcal/mol. Another significant angular distortion in these isomers must reduce these repulsive interactions considerably. The $\text{N}(2)\text{-Co-N}(4)$ angles in both these molecules are expanded: $L\text{-(RSS)}$, 97.0° , 0.7 kcal/mol, and $D\text{-(SRS)}$, 97.8° , 0.9 kcal/mol.

Trien Geometry. Torsional angles about C-N and C-C bonds in the trien rings, calculated from both crystal structure and minimization coordinates, are plotted for the $L\text{-(RRS)}$ and $D\text{-(SSS)}$ isomers (Figure 6). The correlation between experimental observation and prediction from minimization is excellent. The predictive value of the energy minimization is demonstrated by the correlation with torsional angles which are primary parameters in the energy summation (see eq 1), particularly considering the wide range of torsional angles ($12\text{-}53^\circ$) and the large deviations from the strain-free value of 60° .

The close correlation among all four curves would seem to indicate that the trien geometry is almost unaffected by the orientation of the proline molecule in the β_2 isomer system. Further, the agreement between crystal and minimization geometry indicates that intermolecular crystal forces have not significantly perturbed the trien molecular geometry. The evidence from crystal structure analyses,^{12,13,25} nmr,²⁶ molecular models, and minimization calculations on a number of β trien complexes is consistent with a rigid arrangement of the conformations.

(25) H. C. Freeman and I. E. Maxwell, *Inorg. Chem.*, **8**, 1293 (1969).

(26) D. A. Buckingham and A. M. Sargeson, unpublished work.

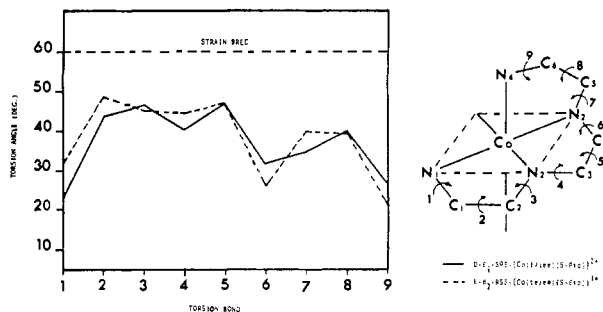


Figure 7. Predicted torsional angles for trien chelate rings: —, calculated from minimized coordinates for $L\text{-}\beta_2\text{-(RSS)-[Co(trien)(S-Pro)]}^{2+}$; ---, calculated from minimized coordinates for $D\text{-}\beta_2\text{-(SRS)-[Co(trien)(S-Pro)]}^{2+}$.

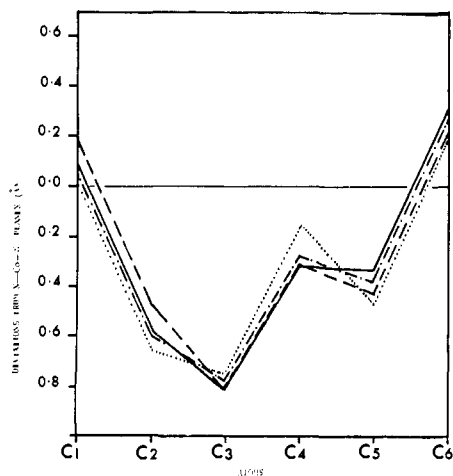


Figure 8. Comparison of deviations of trien chelate ring carbon atoms from their respective N-Co-N planes: —, calculated from minimized coordinates for $D\text{-}\beta_2\text{-(SSS)-[Co(trien)(S-Pro)]}^{2+}$; ---, calculated from crystal structure coordinates for $D\text{-}\beta_2\text{-(SSS)-[Co(trien)(S-Pro)]}^{2+}$; ·····, calculated from minimized coordinates for $L\text{-}\beta_2\text{-(RRS)-[Co(trien)(S-Pro)]}^{2+}$; ·····, calculated from crystal structure coordinates for $L\text{-}\beta_2\text{-(RRS)-[Co(trien)(S-Pro)]}^{2+}$.

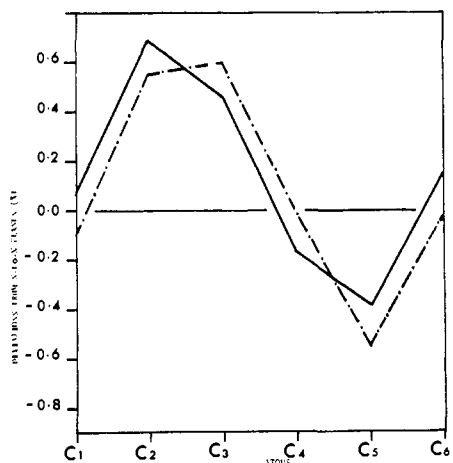


Figure 9. Predicted deviations of trien chelate ring carbon atoms from their respective N-Co-N planes: —, calculated from minimized coordinates for $D\text{-}\beta_2\text{-(SRS)-[Co(trien)(S-Pro)]}^{2+}$; ---, calculated from minimized coordinate for $L\text{-}\beta_2\text{-(RSS)-[Co(trien)(S-Pro)]}^{2+}$.

Figure 7 shows a plot of predicted trien torsional angles calculated from the $L\text{-(RSS)}$ and $D\text{-(SRS)}$ minimized coordinates. Comparison between Figures 6 and 7 shows that inversion at nitrogen N(2) has al-

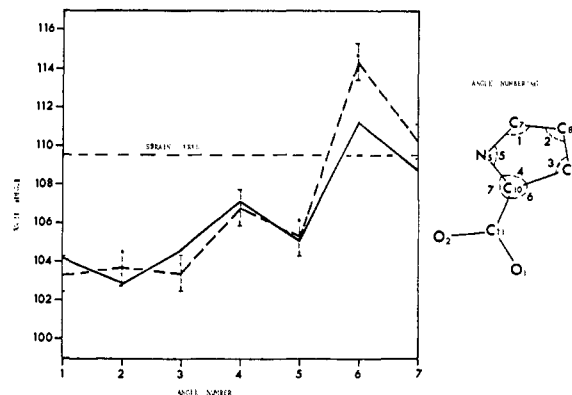


Figure 10. Comparison of bond angles around pyrrolidine of proline: —, calculated from minimized coordinates for $D\text{-}\beta_2\text{-(SSS)-[Co(trien)(S-Pro)]}^{2+}$; ---, calculated from crystal structure coordinates for $D\text{-}\beta_2\text{-(SSS)-[Co(trien)(S-Pro)]}^{2+}$ with standard deviations.

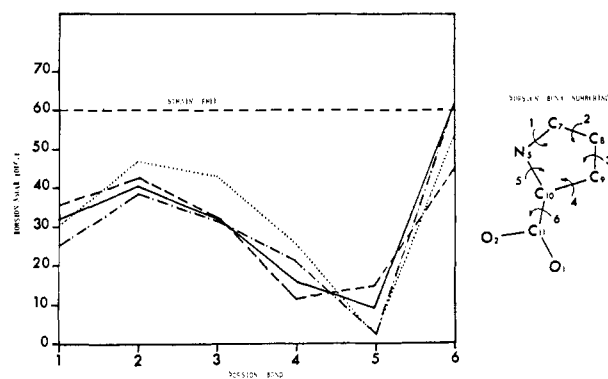


Figure 11. Comparison of torsional angles for the pyrrolidine ring of proline: —, calculated from minimized coordinates for $D\text{-}\beta_2\text{-(SSS)-[Co(trien)(S-Pro)]}^{2+}$; ---, calculated from crystal structure coordinates for $D\text{-}\beta_2\text{-(SSS)-[Co(trien)(S-Pro)]}^{2+}$; ·····, calculated from minimized coordinates for $L\text{-}\beta_2\text{-(RRS)-[Co(trien)(S-Pro)]}^{2+}$; ·····, calculated from crystal structure coordinates for $L\text{-}\beta_2\text{-(RRS)-[Co(trien)(S-Pro)]}^{2+}$.

most no effect on the magnitude of the trien torsion angles with the exception of the torsion angle about the bond N(3)-C(4) which is changed by $\sim 45^\circ$. In Figure 8 the deviations of trien carbon atoms from their respective N-Co-N planes are compared for $L\text{-(RRS)}$ and $D\text{-(SSS)}$, calculated from minimized and crystal coordinates. Figure 9 plots the predicted deviations of carbon atoms from N-Co-N planes for the $L\text{-(RSS)}$ and $D\text{-(SRS)}$ isomers.

A structure of one of the trien isomers of this type is projected, and these β -trien conformational details, along with a comparison of trien coordinated in other geometries, will be discussed in a subsequent publication.

Proline Geometry. The pyrrolidine ring of proline is very strained owing to the restrictions of a five-membered saturated ring system (*cf.* cyclopentane). Some intramolecular bond angles within proline, calculated from $D\text{-(SSS)}$ crystal and minimized coordinates, are plotted in Figure 10. The experimental and predicted values compare well. As expected the internal angles within the pyrrolidine ring are all less than the tetrahedral angle (109.5°) and average at about 105° .

A comparison between torsional angles calculated from crystal and minimized coordinates for $L\text{-(RRS)}$ and $D\text{-(SSS)}$ isomers is given in Figure 11. The agree-

Table IV. Final Energy Terms (kcal/mol) from Minimization

	L- β_2 -(RRS)	D- β_2 -(SSS)	L- β_2 -(RSS)	D- β_2 -(SRS)
Bond length deformations, $\Sigma U(r_{ij})_b$	1.2	1.3	1.5	1.5
Nonbonded interactions, $\Sigma U(r_{ij})_{nb}$	4.7	4.9	5.4	5.8
Valence angle deformations, $\Sigma U(\theta_{ijk})$	7.5	8.9	9.4	11.1
Torsional strain, $\Sigma U(\phi_{ijkl})$	10.3	10.2	10.2	10.5
Total conformational energy, U	23.7	25.3	26.5	28.9
Energy differences (relative to L- β_2 -(RRS))	0	1.6	2.8	5.2

ment between observed and predicted values is very good, more particularly for the D-(SSS) isomer. All the pyrrolidine ring torsion angles are considerably less than the strain-free value (60°). The N(5)-C(10) torsion angle is very small and in the L-(RRS) form this angle reduces to 2° so that the N(5)-C(7) and C(10)-C(9) bonds are virtually eclipsed.

Mean planes, calculated through the pyrrolidine ring for the four minimized molecules and the two crystal structures, show that in all cases the C(8) atom lies ~ 0.6 Å above a plane formed by the other four ring atoms. This deviation is also in the same sense in all instances, namely *trans* to the carboxyl group.

Relative Stabilities of Isomers. The final energy terms from the minimization of each isomer are presented in Table IV. These have been divided into the terms summed in eq 1, nonbonded, $\Sigma_{(ij)} U(r_{ij})_{nb}$; valence, $\Sigma_{(ijk)} U(\theta_{ijk})$; torsional, $\Sigma_{(ijkl)} U(\phi_{ijkl})$; bonded, $\Sigma U_{(ij)}(r_{ij})_b$, and total energy, U .

The calculated energy difference between L-(RRS) and D-(SSS) is 1.6 kcal/mol, and 1.4 kcal/mol of this difference arises from the valence deformation terms. Subsequent to this analysis we discovered that Yoshikawa²⁷ has measured the free energy difference between these two isomers by equilibration on activated charcoal and obtained $\Delta G_{20^\circ} = 1.3$ kcal/mol in favor of the L-(RRS) isomer. The calculated energy difference agrees with this experimental result. It remains to be seen if the energy difference resides in the ΔH term, and some experiments to determine the significance of ΔH and ΔS in equilibria of this nature are in progress.

The calculated and observed energy differences between the isomers are to be compared with that assessed from a consideration solely of nonbonded H \cdots H interactions using the Hill nonbonded potential function²⁸ (~ 14 kcal/mol) and a structure composed from Dreiding models. In the present calculation the difference in nonbonded terms for the two structures is only 0.2 kcal/mol.

The energy differences between the L-(RSS) and D-(SRS) and their parent isomers, L-(RRS) and D-(SSS), are 2.8 kcal/mol and 3.6 kcal/mol, respectively. The results indicate that these isomers might be formed in solution in small concentrations from their parent isomers under mildly basic conditions. However, at present there is no experimental evidence of their existence.

Conclusion

The results show that the energy minimization treatment is successful in predicting the detailed geometries

of the strained β_2 -[Co(trien)(S-Pro)]²⁺ ions. The calculations indicate that angular deformations are important in deciding the relative stabilities of the ions. This is in keeping with past observations that bond angles deform with, comparatively, a small expenditure of energy for quite large angle changes ($\pm 10^\circ$). Also, the angles containing the metal distort in preference to the intraligand angles. Similarly, torsional distortions occur easily and both deformations alleviate close nonbonded interactions. These deviations occur almost to the exclusion of bond length changes. The potential well for bond stretching is steep on both sides while the nonbonded function has one steep barrier as a major constraint to the approach of atoms. In one of the systems examined there is a close balance, particularly between torsional and angular deformations against nonbonded terms, which illustrates the compromise. The results also emphasize that regular models (*e.g.*, Dreiding), although useful for qualitative analyses, are at best crude for any quantitative evaluation of relative stabilities.

The power of the minimization procedure and the independence of the final geometry on the starting coordinates have been demonstrated in the following manner. The D-(SSS) isomer minimized geometry was perturbed such that the new geometry resembled that which would be obtained from a Dreiding model. This required moving the pyrrolidine ring of proline 0.7 Å closer to the apical trien chelate ring ($\Delta x = -0.5$ Å, $\Delta y = 0.5$ Å, $\Delta z = 0$). The minimization procedure shifted the pyrrolidine ring back to a final geometry identical with that of the original minimized structure.

Any contributions from electrostatic or dipole terms have been neglected since we have been unable to evaluate these terms for the coordinated organic molecules. However, the agreement between calculated and observed geometries and relative stabilities implies that the total contribution is small.

Subsequent calculations have shown that the molecular geometry and energy differences are not highly sensitive to the particular choice of force field parameters, and these results will be presented shortly. These studies have also shown that the minimization procedure is not limited to trial coordinates obtained from the structure analyses. We are at present developing procedures for calculating trial coordinates of complex molecules from standard bond lengths, bond angles, and torsional angles. However, it should be emphasized that good trial coordinates reduce the computational time substantially and reduce the possibility of false minima. For the present complexes, the structural coordinates are close to the minimized values, but in other structures some structural deformations are

(27) S. Yoshikawa, private communication.

(28) T. L. Hill, *J. Chem. Phys.*, **16**, 339 (1948).

prescribed by lattice forces which would not be duplicated in the isolated molecule.²⁹

Acknowledgments. We thank Dr. R. H. Boyd for making his minimization program available to us. Also, program ORTEP (Carroll K. Johnson, Oak Ridge,

(29) M. R. Snow, Proceedings of the XIIth International Conference on Coordination Chemistry, Sydney, 1969, p 92.

1965) was used to draw the molecular diagrams for Figures 1 and 4. The calculations were carried out on an IBM 360/50 computer and a CDC-3600 computer. In this regard the assistance of the ANU and CSIRO computer centers is gratefully acknowledged. Drs. M. R. Osborne and G. S. Chandler are thanked for helpful discussions.

Stereochemistry of Tropolonato Complexes Utilizing the Higher Coordination Numbers. I. Nine-Coordinate Tetrakis(tropolonato)-N,N'-dimethylformamidethorium(IV)¹

V. W. Day² and J. L. Hoard³

Contribution from the Department of Chemistry, Cornell University, Ithaca, New York 14850. Received January 6, 1970

Abstract: Molecular crystals of (DMF)ThT₄ (DMF is N,N'-dimethylformamide, T⁻ is the bidentate C₇H₅O₂⁻ tropolonate ion) utilize a two-molecule unit cell, space group P $\bar{1}$, having $a = 15.222$ (9), $b = 10.922$ (6), $c = 9.452$ (5) Å, $\alpha = 113.40$ (1), $\beta = 96.40$ (2), $\gamma = 87.53$ (2)°. The intensities of 7476 independent reflections having $(\sin \theta)/\lambda \geq 0.69$ were measured with Mo K α radiation by the θ - 2θ scanning technique on an automated Picker four-circle diffractometer; the 6792 data statistically retained as observable were employed for structure determination and anisotropic refinement to an R of 0.047; all hydrogen atoms were directly placed. The nine-coordinate (DMF)-ThT₄ molecule in the crystal approximates closely to C_s-m symmetry; it occurs as one of seven theoretical stereoisomers that utilize the monocapped square antiprism as coordination polyhedron. One tropolonato ligand spans a slant edge of the pyramidal cap while the monodentate ligand takes the one other vertex, also in the cap, that allows retention of C_s symmetry. A second tropolonato ligand spans the basal edge of the polyhedron opposite to the monodentate ligand, and the two other tropolonato ligands span a mirrored pair of lateral edges of the polyhedron. Dimensional variations from the ideal C_{4v} geometry of the polyhedron are required by the small "bite" of the tropolonato ligand (2.52–2.56 Å); inter-ring O...O contacts range upward from 2.79 Å. The length of the Th–O bond to the apical oxygen, 2.485 (5) Å, is significantly greater than the average, 2.445 Å, for the other seven bonds to tropolonato oxygen; the bond to the uncharged DMF ligand at 2.519 (6) Å is still longer. Bond parameters in the tropolonato ligands compare favorably with those reported from simpler structures.

Stable mononuclear complexes that utilize coordination numbers greater than six are predominantly chelated species. It is, nonetheless, the configurational geometries theoretically attainable with monodentate ligands that provide the most illuminating basis for the stereochemical discussion of experimentally preparable complexes. The geometry of packing N spherically symmetric, chemically identical, monodentate ligands around a central cation affords a decisive preference for a particular coordination polyhedron when N is 4, 6, or 12, corresponding to any one of the three regular polyhedra with triangular faces (tetrahedron, octahedron, and icosahedron). In Figure 1 the ratio (ρ) of polyhedron radius or complexing bond length (M–L) to polyhedron edge length or ligand packing diameter (L–L) is plotted against coordination number (N) for the more probable coordination polyhedra.⁴ Points

representing the three regular polyhedra with triangular faces and the three-coordinate equilateral triangle define the straight line that represents a uniformly excellent stereochemistry; for a fixed ligand diameter or polyhedron edge length (L–L), the slope of this line gives the fractional increment in the complexing bond length (M–L) with unit increase in the coordination number (N) that maintains steric excellence. It is evident that the transition from the octahedron to the best of the seven-coordination polyhedra is not taken easily, whereas the step from seven- to eight-coordination (the cube excluded) is a small one. Within the wide gap separating the octahedron and the icosahedron, the better eight- and nine-coordination polyhedra are approximately equal in steric merit, as are also, at a lower level of merit, the better seven- and ten-coordination polyhedra.

For each of the coordination numbers, five and seven-ten inclusive, there are two (at least) coordination polyhedra that differ radically in symmetry type, but only modestly in the value of (M–L)/(L–L). Each

(1) This investigation was supported in part by National Science Foundation Grant No. GP-6710X, by Public Health Research Grant No. 2-RO1-GM09370 from the National Institutes of Health, General Medical Sciences, and by the Advanced Research Projects Agency.

(2) National Science Foundation Predoctoral Trainee, 1965–1969.

(3) Author to whom correspondence should be addressed.

(4) Figure 1 is an alternative, easily grasped representation of the Pauling minimum radius ratios for the stability of various coordination polyhedra;⁵ it is empirically useful irrespective of the nature of the complexing bonds.

(5) L. Pauling, "The Nature of the Chemical Bond," 3rd ed, Cornell University Press, Ithaca, N. Y., 1960, pp 544–546. Pauling has employed his "univalent" ionic radii for the prediction of maximum coordination numbers with marked success.⁶

(6) L. Pauling, *J. Amer. Chem. Soc.*, **55**, 1895 (1933).